

Supplementary Material: **Impacts of the changing ocean-sea ice system on the key forage fish Arctic cod (*Boreogadus Saida*) and subsistence fisheries in the Western Canadian Arctic - Evaluating linked climate, ecosystem and economic (CEE) models**

1 SUPPLEMENTARY INFORMATION ON MODELS

The presented manuscript includes a sequence of model tools, i.e. climate models to assess environmental changes based on different global emission scenarios, and a dynamic bioclimatic envelope model to assess potential changes in species distribution and abundance based on those environmental changes. In the following we are providing supplementary details on those model tools.

1.1 Domain and Forcing for the NAA-CMOC and NAA-CanOE-CSIB models

The domain, bathymetry and resolution of the regional Arctic ocean sea-ice-biogeochemistry models NAA-CMOC and NAA-CanOE-CSIB models are indicated in Fig S1. The horizontal resolution ranges from 10 to 14.5km with highest resolution in the Canadian Arctic. The bathymetry is based on the International Bathymetric Chart of the Arctic Ocean (IBCAO). The bathymetry provides a reasonable representation of the larger scale features in the Arctic, however small scale near coastal areas are only limitedly charted in the Arctic and lack in detail.

The initial ocean temperatures and salinities are set from the Polar Hydrographic Climatology (PHC3.0) (http://psc.apl.washington.edu/nonwp_projects/PHC/Climatology.html, updated from Steele et al., 2001) for NAA-CMOC and set to ORAS4 1969 January data for NAA-CanOE-CSIB. The initial DIC, ALK, and NO₃ were taken from annual GLODAP v2b climatology data (1972-2013) (<http://cdiac.ornl.gov/oceans/GLODAPv2/> Lauvset et al., 2016). Other biogeochemical open boundary fields were assigned constants.

The model simulation was conducted by prescribing annually-varying surface and lateral boundary conditions. The surface boundary conditions for the hindcast are based on the Drakkar Forcing Set 5.2 (DFS, Dussin et al., 2016). Seawater temperature, salinity, and horizontal currents at the Pacific and Atlantic lateral open boundaries of the model domain were prescribed using the interannual monthly-mean fields based on the Ocean Reanalysis System 4 (Balmaseda et al., 2013, ORAS4). River discharge of freshwater was prescribed based on the monthly-mean product (Dai and Trenberth, 2002), which covers the period up to 2007. Due to the absence of the data product beyond 2007, the monthly-mean fields for 2007 were prescribed repeatedly beyond this year in the model simulation. A detailed description with in dept discussions of forcing and model output can be found in Hayashida (2018).

To drive future projections under RCP8.5 for the years 2006 to 2085, the 22km resolution Canadian Regional Climate Model version 4 (CanRCM4) (Scinocca et al., 2015) covering the Coordinated Regional Climate Downscaling Experiment (CORDEX) Arctic domain was merged with output from the Canadian

earth system model version 2 (CanESM2) where CanRCM4 does not fully cover the NAA domain to create a forcing data set for the NAA-CMOC model. Daily surface wind forcing was applied as is, while anomalies have been calculated for all other variables (daily snow fall, air temperature (at 10 m), longwave, shortwave, liquid precipitation and specific humidity). The anomalies are calculated combining the merged CanESM2-CanRCM4 dataset with the Coordinated Ocean-ice Reference Experiments (CORE2) dataset (http://data1.gfdl.noaa.gov/nomads/forms/core/COREv2/code_v2.html Large and Yeager, 2004, 2009) for the reference period 1986-2005, following the approach of (Dumas et al., 2003). Ice thickness, ice concentration and snow thickness were initialized from a five year run with repeated 2006 anomaly forcing. River runoff was derived from observations (Dai and Trenberth, 2002; Dai et al., 2009) with river DIC from Tank et al. (2012) representing coastal and river runoff (no changes were applied for future timeperiods). Monthly timeseries open boundary conditions were derived from CanESM2 model output by linearly interpolating between the climatological means from 1986-2005 (representing 1996), 2006-2025 (representing 2016) and 2066-2085 (representing 2076).

1.2 Evaluation of the NAA-CanOE-CSIB model simulation

Results of the NAA-CanOE-CSIB model simulation over the recent past (1979-2015) have been evaluated via comparison with observational and other model data products in Hayashida (2018). However, the evaluation focused on the mean state and trend over the Arctic as a whole and did not discuss regional variability. Hence, here we include a model evaluation focusing on the Western Canadian Arctic via comparison of ice concentration, ice-algal productivity, and sea-surface chlorophyll-*a* concentration with satellite-derived and other model data products.

1.2.1 Ice concentration

Modelled ice concentration is compared with the satellite-derived data product (Peng et al., 2013; Meier et al., 2017) based on the combination of the well-established algorithms: the NASA Team algorithm (Cavalieri et al., 1984) and NASA Bootstrap algorithm (Comiso, 1986). Figure S2 shows the modelled spatial pattern that is consistent with the satellite-derived data product for both the spring and summer seasons. The discrepancies between the model and the satellite-derived product are generally larger in the summer than in the spring (S2C,G). In particular, the modelled ice concentration is higher than the satellite-derived product along the northern rim of the Baffin Bay in the spring and along the Beaufort Shelf in the summer. On the other hand, the modelled ice concentration is lower than the satellite-derived product especially along the coast near the McKenzie river in the spring and in the Beaufort Basin near the limit of satellite coverage (as indicated by blank) and at various locations in the Canadian Polar Shelf in the summer. The linear trends in the satellite-derived product over 1979-2015 are shown in Figure S2D,H, which generally resemble the patterns derived from the model simulation (main manuscript, Figure 4C,I). The only discrepancies are along the northern rim of the Baffin Bay for both the spring and summer as well as part of the Beaufort Gyre in the summer.

1.2.2 Ice-algal productivity

Modelled ice-algal productivity and key environmental variables are analyzed in detail in the multi-model intercomparison study on pan-Arctic ice-algal productivity (Watanabe et al., 2019). The study focuses on the mean state and trend over the three decades (1980-2009) simulated by the five participating models. Here, we summarize the outcome of the study within the context of the Western Canadian Arctic. Modelled ice-algal productivity in the Western Canadian Arctic simulated by the NAA-CanOE-CSIB model is consistent with the majority of the participating models. The productivity is very high ($>20 \text{ mmol-N m}^{-2}$

per year) in the Canadian Polar Shelf and Beaufort Shelf, which is consistent with the two other models. On the other hand, the productivity is low ($<5 \text{ mmol-N m}^{-2}$ per year) in the Beaufort Sea, which is consistent with the three other models. The ice-algal productivity in this region is significantly anti-correlated (the correlation coefficient of -0.48) with snow depth, which is unique to the NAA-CanOE-CSIB model.

1.2.3 Sea-surface chlorophyll a concentration

The spatial distribution of modelled sea-surface chlorophyll a concentration averaged over 1997-2010 is compared with the satellite-derived product of the Sea-viewing Wide Field-of-view Sensor (SeaWiFS) Ocean Color Data (S3). The model and the satellite-derived product generally agree that the chlorophyll-*a* concentration is high on the Beaufort Shelf where ice concentrations are relatively low (S2), reducing light limitation. However, they differ greatly in magnitude with the satellite-derived product showing much higher values (up to 40 and 90 mg-Chl*a* m^{-3} in the spring and summer, respectively). These high values are well known to be a bias in the satellite-derived product due to the presence of terrestrial coloured dissolved organic matter (CDOM) and suspended matter injected from the McKenzie River (Mustapha et al., 2012). Another area where the satellite-derived product shows higher values than the model is along the narrow channel between the Canadian Arctic Archipelago and Greenland (S3C,F). In other regions the model tends to simulate higher values than the satellite-derived product especially in the Canadian Polar Shelf. Note that integrated Chl-*a* estimates are difficult to obtain from satellites, since the satellite sensors are not able to detect subsurface Chl-*a* maxima which are ubiquitous in the Arctic (Ardyna et al., 2013).

1.3 The Dynamic Bioclimatic Envelope Model (DBEM)

Details of the original dynamic bioclimatic envelope model (DBEM) can be found in (Cheung et al., 2008, 2011, 2016). Here we provide a basic overview of the main components of the model, how these components link to one another (Figure S2), and summarize the applicable details that pertain to this study.

Initial species distributions were taken from the Sea Around Us database, which uses a number of set criteria to generate the spatial distribution of each species on a 0.5° longitude by 0.5° latitude grid (further details can be found at <http://www.seararoundus.org/>). The sequence of steps were as follows: 1) species were restricted based on observations in statistical areas defined by the United Nations Food and Agricultural Organization (FAO); 2) distributions were restricted by a northern and southern latitudinal range based on observations and literature; 3) an expert reviewed range-limiting polygon was overlaid to further confine species distributions to known areas; and 4) distributions were further limited based on depth range, habitat preference (e.g. coral, seagrass, estuaries, sea ice), and equatorial submergence. Habitat preference data were primarily collected from FishBase (Froese and Pauly, 2018) and SeaLifeBase (Palomares and Pauly, 2018).

Habitat suitability and environmental preferences were determined by using initial species distribution maps and overlaying environmental parameters from earth system model outputs (e.g. temperature, salinity, depth, sea ice, dissolved oxygen). Species-specific parameters on habitat affinity (e.g. coral, sea ice, seagrass) were also incorporated to characterize the bioclimatic envelope. Initial environmental conditions are assumed to be the average conditions between years 1971 and 2000. A major assumption in the model is that each spatial cell of the initial distribution is at carrying capacity at time zero. Carrying capacity is positively correlated with habitat suitability and will thus change as the environment changes (Cheung et al., 2011). Populations move based on gradients of environmental suitability and carrying capacity, and we can expect populations to shift in space and time to optimize areas where habitat is more suitable and potential for population growth is higher (for details on the equations see Cheung et al., 2011; Tai et al., 2018). Dispersal for larvae was modelled using an advection-diffusion model and a pelagic duration

model. As a result larval dispersal and recruitment were determined by oceanic currents (obtained from earth system model outputs), diffusivity, and the duration spent as pelagic larvae. Net adult migration was determined by the geographical distance between the centres of adjacent cells, the relative size of a species (e.g. small reef-dwelling, large-bodied pelagics), and a fuzzy logic model based on differences in habitat suitability between surrounding neighbour cells (Cheung et al., 2008). Therefore, there will be a net emigration if surrounding cells are more favourable, and a net immigration if the present cell is preferable to surrounding cells.

Individual growth was modelled using a derived version of the von Bertalanffy growth function to incorporate the gill-oxygen limitation hypothesis (Pauly and Cheung, 2017) and oxygen- and capacity-limited thermal tolerance hypothesis (Pörtner and Lannig, 2009) to model ecophysiological responses to temperature, acidity, and oxygen. I.e. the model assumes that physiological stressors (i.e., temperature, pH, oxygen supply), such as deviations from the optimal temperature, act to reduce aerobic scope and thus the energy available for growth (Pörtner, 2010). The model is grounded on the theory that oxygen supply is limiting post-larval fish growth and reproduction for marine fish and invertebrates and changes to environmental conditions can alter the oxygen supply-demand dynamics and various life history processes and traits (Cheung et al., 2011; Pauly and Cheung, 2018). Ocean acidification and changes in dissolved oxygen concentration were modeled to act synergistically with temperature and shrink the overall aerobic scope (Cheung et al., 2011; Pörtner and Farrell, 2008). Ocean acidification was also modeled as a correlative process to affect survival (Tai et al., 2018). Population growth was then modelled using the logistic growth function (Hilborn and Walters, 1992).

1.4 Figures

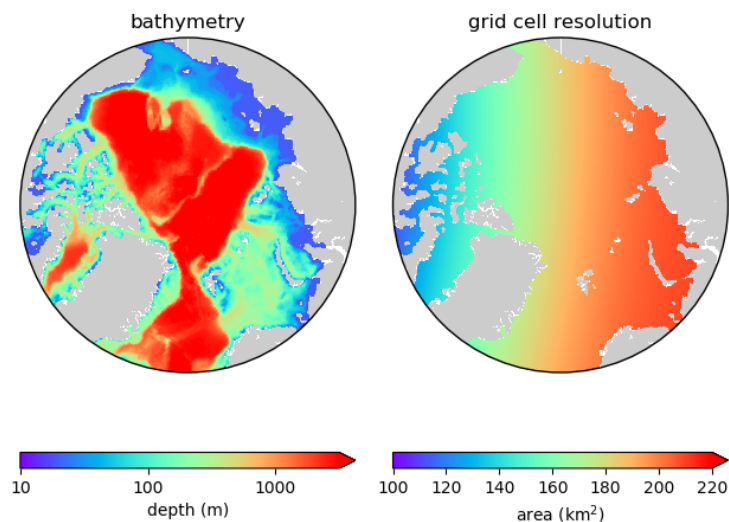


Figure S1. Domain and resolution of the regional Arctic ocean sea-ice-biogeochemistry models NAA-CMOC and NAA-CanOE-CSIB models

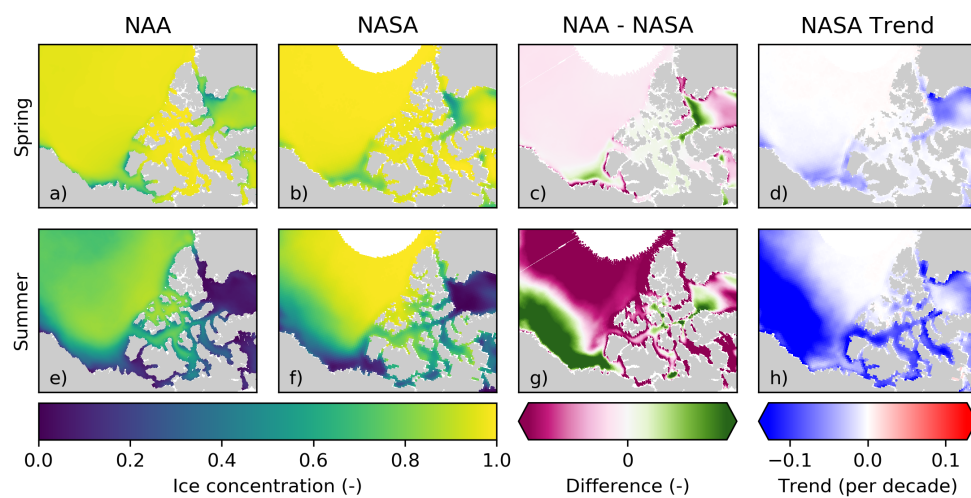


Figure S2. Spring (April-June; A, B) and summer (July-September; E, F) ice concentration fields based on the NAA-CanOE-CSIB model simulation (NAA; A, E) and the satellite-derived product (NASA; B, F) averaged over 1979-2015, their respective differences (NAA - NASA; C, G), and their linear trends in the Western Canadian Arctic. The colorbar scale for D and H is adjusted to match with that of Figure 4 in the main manuscript. For C and G only, the satellite-derived product is interpolated onto the model grid.

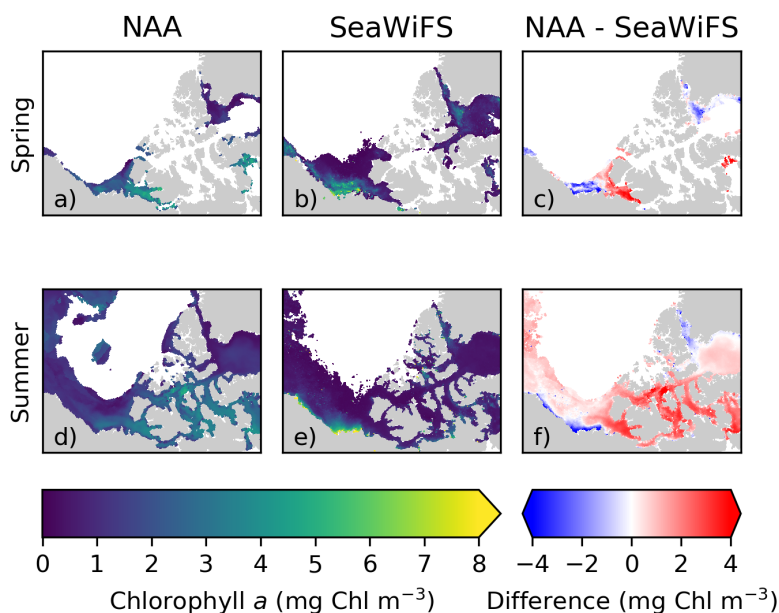


Figure S3. Spring (April-June; A, B) and summer (July-September; D, E) sea-surface chlorophyll-*a* concentration fields based on the NAA-CanOE-CSIB model simulation (NAA; A, D) and the satellite-derived product (SeaWiFS; B, E) averaged over 1997-2010, and their respective differences (NAA - SeaWiFS; C, F) in the Western Canadian Arctic. For C and F only, the satellite-derived product is interpolated onto the model grid. For A and B, the blank denotes ice-covered regions where no data are detected via remote sensing. For D and E, the blank denotes ice-covered regions where ice concentration exceeds 0.15 throughout 1997-2010 in the model.

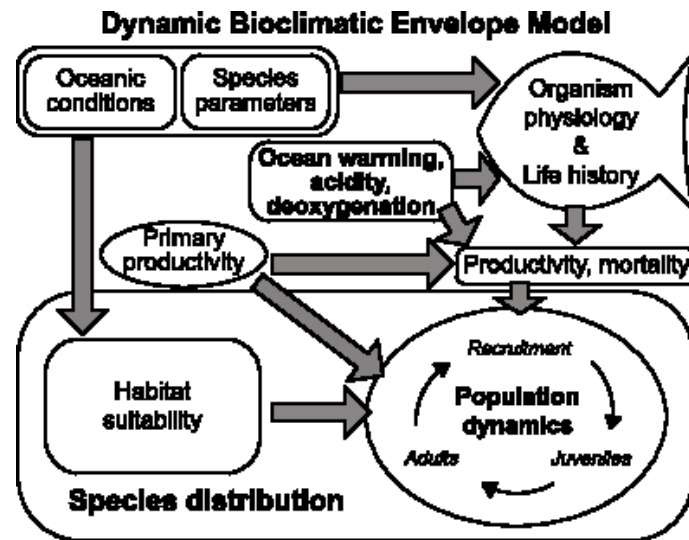


Figure S4. Conceptual diagram of the dynamic bioclimatic envelope model indicating the components and connections within the model. Grey arrows indicate direction of input.

REFERENCES

- Ardyna, M., Babin, M., Gosselin, M., Devred, E., élarger, S. B., Matsuoka, A., et al. (2013). Parameterization of vertical chlorophyll a in the arctic ocean: impact of the subsurface chlorophyll maximum on regional, seasonal, and annual primary production estimates. *Biogeosciences* 10. Doi:10.5194/bg-10-4383-2013
- Balmaseda, M., Mogensen, K., and Weaver, A. (2013). Evaluation of the ECMWF ocean reanalysis system oras4. *Quarterly Journal of the Royal Meteorological Society* 139, 1132–1161
- Cavaliere, D., Gloersen, P., and Campbell, W. (1984). Determination of sea ice parameters with the nimbus 7 smmr. *J. Geophys. Res* 89, 5355–5369. Doi:10.1029/JD089iD04p05355.
- Cheung, W., Dunne, J. P., Sarmiento, J. L., and Pauly, D. (2011). Integrating ecophysiology and plankton dynamics into projected maximum fisheries catch potential under climate change in the Northeast Atlantic. *ICES Journal of Marine Science* 68, 1008–1018
- Cheung, W., Jones, M., Reygondeau, G., Stock, C., Lam, V., and Froelicher, T. (2016). Structural uncertainty in projecting global fisheries catches under climate change. *Ecol. Modell.* 325, 57–66. Doi:10.1016/j.ecolmodel.2015.12.018
- Cheung, W., Lam, V. W., and Pauly, D. (2008). Modelling present and climate-shifted distribution of marine fishes and invertebrates. *Fish. Cent. Res. Reports* 16
- Comiso, J. (1986). Characteristics of arctic winter sea ice from satellite multispectral microwave observations. *J. Geophys. Res.* 91, 975–994. Doi:10.1029/JC091iC01p00975
- Dai, A., Qian, T., Trenberth, K., and Milliman, J. D. (2009). Changes in continental freshwater discharge from 1948-2004. *J. Climate* 22, 773–2791
- Dai, A. and Trenberth, K. (2002). Estimates of freshwater discharge from continents: Latitudinal and seasonal variations. *J. Hydrometeorol.* 3, 660–687
- Dumas, J., Flato, G., and Weaver, A. (2003). The impact of varying atmospheric forcing on the thickness of arctic multi-year sea ice. *Geophysical Research Letters* 30. <https://doi.org/10.1029/2003GL017433>
- Dussin, R., Barnier, B., Brodeau, L., and Molines, J. (2016). *The making of the Drakkar Forcing Set DFS5*. Tech. Rep. 01-04,16, DRAKKAR/MyOcean
- [Dataset] Froese, R. and Pauly, D. (2018). Fishbase. World Wide Web electronic publication. www.fishbase.org, version (02/2018)
- Hayashida, H. (2018). *Modelling sea-ice and oceanic dimethylsulfide production and emissions in the Arctic*. Ph.D. thesis, School of Earth and Ocean Sciences, University of Victoria
- Hilborn, R. and Walters, C. (1992). *Quantitative Fisheries Stock Assessment*. (Boston, MA: Springer US). Doi:10.1007/978-1-4615-3598-0
- Large, W. and Yeager, S. (2004). *Diurnal to decadal global forcing for ocean and sea-ice models: the datasets and flux climatologies*. Tech. Rep. TN-460+ STR, National Center for Atmospheric Research (NCAR)
- Large, W. and Yeager, S. (2009). Core2: The global climatology of an interannually varying air-sea flux data set. *Climate Dyn* 33, 341–364
- Lauvset, S., Key, R., Olsen, A., van Heuven, S., Velo, A., Lin, X., et al. (2016). A new global interior ocean mapped climatology: the 1°x1° glodap version 2. *Earth Syst. Sci. Data* 8, 325–340. <https://doi.org/10.5194/essd-8-325-2016>
- [Dataset] Meier, W., Fetterer, F., Savoie, M., Mallory, S., Duerr, R., and Stroeve, J. (2017). Noaa/nsidc climate data record of passive microwave sea ice concentration, version 3. Boulder, Colorado USA. NSIDC: National Snow and Ice Data Center. Doi: <https://doi.org/10.7265/N59P2ZTG>, Accessed 02/25/2019

- Mustapha, S., Bélanger, S., and Larouche, P. (2012). Evaluation of ocean color algorithms in the southeastern beaufort sea, canadian arctic: New parameterization using seawifs, modis, and meris spectral bands. *Canadian Journal of Remote Sensing* 38, 535–556. DOI: 10.5589/m12-045
- [Dataset] Palomares, M. and Pauly, D. (2018). Sealifebase. World Wide Web electronic publication. [Www.sealifebase.org](http://www.sealifebase.org)
- Pauly, D. and Cheung, W. (2017). Sound physiological knowledge and principles in modeling shrinking of fishes under climate change. *Global Change Biology* , 1–12
- Pauly, D. and Cheung, W. (2018). Sound physiological knowledge and principles in modeling shrinking of fishes under climate change. *Glob Change Biol* 24, e15–e26. DOI: 10.1111/gcb.13831
- Peng, G., Meier, W., Scott, D., and Savoie, M. (2013). A long-term and reproducible passive microwave sea ice concentration data record for climate studies and monitoring. *Earth Syst. Sci. Data.* 5, 311–318. [Https://doi.org/10.5194/essd-5-311-2013](https://doi.org/10.5194/essd-5-311-2013)
- Pörtner, H. O. (2010). Oxygen- and capacity-limitation of thermal tolerance: a matrix for integrating climate-related stressor effects in marine ecosystems. *Journal of Experimental Biology* 216, 881–893
- Pörtner, H. O. and Farrell, A. P. (2008). Ecology, physiology and climate change. *Science* 322, 690–692. Doi:10.1126/science.1163156.
- Pörtner, H. O. and Lannig, G. (2009). *Fish Physiology* (Burlington: Elsevier Inc.), chap. Oxygen and Capacity Limited Thermal Tolerance. 1 edn. Doi:<http://dx.doi.org/10.1016/S1546>
- Scinocca, J., Kharin, V., Jiao, Y., Qian, M., Lazare, M., Solheim, L., et al. (2015). Coordinated global and regional climate modelling. *Journal of Climate*
- Steele, M., Morley, R., and Ermold, W. (2001). Phc: a global ocean hydrography with a high-quality arctic ocean. *Journal of Climate* 14, 2079–2087
- Tai, T., Harley, C., and Cheung, W. (2018). Comparing model parameterizations of the biophysical impacts of ocean acidification to identify limitations and uncertainties. *Ecological Modelling* 385, 1–11. Doi:<https://doi.org/10.1016/j.ecolmodel.2018.07.007>
- Tank, S. E., Raymond, P. A., Striegl, R. G., McClelland, J. W., Holmes, R. M., Fiske, G. J., et al. (2012). A land-to-ocean perspective on the magnitude, source and implication of dic flux from major Arctic rivers to the Arctic Ocean. *Global Geochemical Cycles* 26. Doi:10.1029/2011GB004192
- Watanabe, E., Jin, M., Hayashida, H., Zhang, J., and Steiner, N. (2019). Multi-model intercomparison of the pan-arctic ice algal productivity on seasonal and decadal timescales. *JGR Oceans*